Effective *R*-value approach to comprehend the essence of integrated opaque passive substrate properties

Kishor T. ZINGRE, D.E.V.S. Kiran KUMAR, Man Pun WAN, Christopher.YH. CHAO

PII: S2352-7102(21)00723-3

DOI: https://doi.org/10.1016/j.jobe.2021.102865

Reference: JOBE 102865

To appear in: *Journal of Building Engineering*

Received Date: 15 December 2020

Revised Date: 5 June 2021

Accepted Date: 7 June 2021

Please cite this article as: K.T. ZINGRE, D.E.V.S. Kiran KUMAR, M. Pun WAN, C.Y. CHAO, Effective *R*-value approach to comprehend the essence of integrated opaque passive substrate properties, *Journal of Building Engineering*, https://doi.org/10.1016/j.jobe.2021.102865.

Authors Statement

Zingre, K. T.: Conceptualization, Formal analysis, Writing-original draft preparation

Kumar, D. E. V. S. K: Conceptualization, Formal analysis, Writing-original draft preparation

Wan, M. P.: Conceptualization, Supervision. Writing-review & editing, funding acquisition,

Chao, C. Y. H.: Supervision, funding acquisition

All authors have read and agreed to the published version of the manuscript.

Effective *R*-value approach to comprehend the essence of integrated opaque passive substrate properties

Kishor T. ZINGRE[a,*], D. E. V. S. Kiran KUMAR[b,c], Man Pun WAN[b,c], Christopher Y. H. CHAO[d]

[a]*Department of Architecture and Built Environment, Northumbria University, Newcastle, United Kingdom.*
[b]*Energy Research Institute at NTU, Nanyang Technological University, Singapore*
[c]*School of Mechanical and Aerospace Engineering, Nanyang Technological University, Singapore*
[d]*Department of Mechanical Engineering, University of Hong Kong, Hong Kong*

Corresponding author: Dr. Kishor T. ZINGRE, Tel.: +44 7774649415.
Email: Kishor.Zingre@northumbria.ac.uk

Abstract

The concept of 'effective' thermal resistance could facilitate in-depth understanding of the impact of passive substrate properties such as surface radiative and thermo-physical (which are not directly measurable using instrumentations in terms of *R*-value). A simple to-use and concise single performance factor has been formulated in this study to comprehend the effective thermal resistance provided by the enhanced surface radiative and thermo-physical properties of passive envelope materials. The derived expression is validated against measurements in real residential apartments located in Singapore. The derived effective thermal resistance expression is function of solar radiative properties, thermo-physical properties and weather parameters, and hence contains much more information than the traditionally estimated R-value. The effective thermal resistance is found to be dynamic in behaviour i.e., thermal resistance (or heat flow character) of the envelope material varies with transient weather conditions. Increasing roof surface radiative properties i.e., solar reflectance (from 0.1 to 0.8) alone has advantages during both daytime and nighttime with daily integrated-heat gain reduction by 60-68%. Whereas increasing the other thermo-physical properties of the envelope i.e., adding insulation or thermal mass (with a layer of phase change material-modified skim coat) has advantage only during daytime, but penalty during nighttime for the hot climates. The effect of increasing the solar reflectance by 0.7 for an insulated gray aluminum metal roof (with 20-mm polystyrene) is almost equivalent to effectively further adding 40-mm thick polystyrene. The application of proposed approach has been demonstrated by investigating the effect of passive envelope properties for different roof assemblies under four different climates. Using this approach, the accuracy of estimation of heat flux through roof, an indicator of the roof thermal efficiency, which was found to have improved by up to 78% against commonly found any steady-state method of heat flux estimation.

Keywords: Effective *R*-value, passive envelope efficiency; heat transfer modelling; radiative properties; cool materials.

1. Introduction

Solar radiation incident on the surface of opaque building fabric (e.g., a roof or a wall) gets partially absorbed by the building fabric. A portion of this absorbed heat is stored in the building material and the residual portion is transferred to the indoor environment, adding to the heat load of the building [1-2]. In hot climates, popular strategies that aim to reduce the heat gain through opaque (non-glazing) part of building envelope include: i) increasing surface albedo (ρ) to reflect back the incoming solar radiation, ii) raising thermal resistance or *R*-value (*R* hereafter) to minimize the conduction heat gain and iii) increasing volumetric heat capacity (C_v) to increase the capacity of heat storage in the building fabric material for daytime and release some of the stored heat to outdoors during night-time [3]. Strategy i) could be realized by applying a high solar reflectance material, e.g., using high albedo coatings on the exterior surfaces of the building [1]. Strategy ii) could be achieved by adding insulation material or incorporating an air gap in between the material layers, e.g., double-skin roof, [4]. Strategy iii) could be achieved by adding thermal inertia, e.g., using thicker material or materials of higher densities, or adding phase change material into the building fabric assemblies [3]. These passive substrate strategies are particularly essential in tropical climate regions where the solar radiation intensity is usually high [3-4].

Cool roof coatings have properties of high solar reflectance ($\rho > 0.65$) and thermal emittance ($\varepsilon > 0.75$), to enhance the reflection of incident solar radiation and the re-emission of stored heat [5]. Recent studies on cool coatings found that these strategies are effective in reducing heat gain into buildings, but their performance varies with the climate conditions [5-6]. Zingre et al. [7] suggested that increasing envelope thermal efficiency due to the addition of cool coating can be characterized as an 'effective' increase in the thermal resistance of the building fabric assembly. The effective thermal resistance increment is a notional concept which represents the increase in thermal resistance that would result in an effective improvement in the thermal performance (i.e., reduced heat gain), as that caused by a high surface reflectance. Unlike insulation materials which have constant thermal resistance, the 'effective' thermal resistance of cool roof coatings and phase change materials exhibits a dynamic characteristic as weather condition changes with time. In this study, dynamic behavior of opaque passive substrate properties (such as surface radiative and thermo-physical) are investigated by taking into account their integrated effect using effective *R*-value approach.

2. Review of previous studies

As pointed out by Kosny et al. [6] and Muscioa & Akbari [8], the existing guidelines/codes adopted in several countries to improve thermal efficiency of building envelopes such as ASHRAE standards 90.1 in the USA [8], EPBD in Europe [6] and BCA's ETTV in Singapore [9-10], do not necessarily factor-in the dynamic thermal behavior of opaque passive substrate properties (as summarized in Table 1). It is because these codes are primarily based on steady-state thermal properties of building fabric assemblies. There is a need to formulate new expressions for dynamic effective thermal resistance increment (provided by the passive strategies) under transient weather conditions and incorporating into the existing codes, as discussed in [6-8, 10]. Experimental [11-12] and numerical [13-24] studies on the effective thermal resistances due to various passive strategies such as green roof, ventilated roof and insulation roof were reported. However, the results of these studies are limited to specific building materials, wall configurations, indoor/outdoor boundary conditions etc., restricting their general applicability to integrated properties e.g., combination of cool coating with phase change material or air-cavities, as discussed in [16]. Mathematical models aiming to overcome these limitations were developed [25-26] using inverse and optimization methods. However, these models [25-26] themselves are also subjected to other limitations including i) being too complicated to implement in practice, ii) lacking experimental validations and iii) adopting certain approximations for the estimation of surface heat transfer coefficients. In some other studies, multiplier coefficients and mathematical indices were derived based on steady-state analysis, limiting their applicability to buildings subjected to transient boundary conditions [27]. A set of simple and easy-to-implement numerical models for evaluating dynamic thermal behavior of integrated passive substrate properties i.e., surface reflectance, thermal mass together with the thermal insulation properties of the envelope material under different weather conditions is utmost important to building designers to quantify its thermal and energy impacts, especially in the design stage.

This study aims at formulating a novel analytical expression for accurate estimation of effective dynamic thermal resistance provided by opaque passive substrate materials i.e., building envelope covered with cool and phase change materials. The proposed model (illustrated in Table 1), on one hand overcomes the drawbacks of the existing methodologies [6, 8-10] that are limited to steady-state thermal resistance of building materials and on the other hand, applicable to both roof and wall. The proposed numerical expression is generally applicable to: i) any envelope (roof and wall) surfaces, ii) any envelope materials and iii) any

climate conditions. The applicability of the model is demonstrated using field experiments conducted at two adjacent apartment units in a 12-storey building in Singapore.

Table 1 Comparison of various methods to incorporate effect of passive substrate properties in thermal efficiency of building envelope.

Method / Approach	Source	Approach for building fabric assemblies	Formulation	Features
New (proposed)	**This study**	- Dynamic thermal resistance - Incorporates the effect of enhanced radiative and thermo-physical properties	$R_{\rho^*}^{new} = \bar{R}_o + \bar{R}_{substrate} + \bar{R}_i + \bar{R}_{\rho^*}^{CRHT}$	- Applicable to transient boundary conditions - Applicable to opaque walls and roof - Applicable to any substrate material - Applicable to any climate
Existing	[8, 10]	- Steady-state thermal resistance - No effect of enhanced radiative and thermo-physical properties	$R_{\rho^*} = \bar{R}_o + \bar{R}_{substrate} + \bar{R}_i$ (based on assumption $\bar{R}_{\rho^*}^{CRHT} = 0$)	-Applicable to only steady state boundary conditions

The new contributions of this study include: 1) formulation of an analytical model to study in-depth dynamic (hourly basis) variation in the R-value due to passive substrate properties (including their surface radiative and thermal mass properties), 2) Potential modifications to the current worldwide building codes which are based on steady-state analysis and 3) generalized expression which is applicable to any envelope assembly and climatic conditions which can be readily used for accurate estimation of envelope thermal efficiency parameter such as heat flow, with an approach aimed at ease of calculations and not restricted by climate conditions or dynamic behavior of envelope substrate material.

3. Formulation of analytical model for effective *R*-value, $\bar{R}_{\rho^*}^{CRHT}$

The approach of effective thermal resistance which integrates the enhanced surface radiative (such as solar reflectance and thermal emittance) and thermo-physical properties (such as thermal resistance and thermal inertia), could facilitate to study the effectiveness of high reflectance/emittance/heat capacity coating on top of a conventional roof (an imaginary opaque solid roof or 'gray roof' hereinafter). An expression for single performance factor, $\bar{R}_{\rho^*}^{CRHT}$ is proposed in terms of heat fluxes through the roof (with solar reflectance of ρ^*) and the same gray roof (with solar reflectance of ρ).

The heat flux through a reference gray roof (based on the heat transfer model [28-29]) is given by,

$$q_{\rho}^{CRHT} = U_{\rho}\,(1+\nu)\left\{T_{sol-air}^{S} - \left[T_i\left(1-\frac{U_{\rho}}{h_o}\right)+\left(\frac{U_{\rho}}{h_o}\right)T_{sol-air,M}\right]\right\}_{\rho} \tag{1}$$

$$= U_{\rho}\left(TD_{\rho}^{eqv}\right) \tag{1a}$$

where $\left(TD_{\rho}^{eqv}\right) = (1+\nu)\left\{T_{sol-air}^{S} - \left[T_i\left(1-\frac{U_{\rho}}{h_o}\right)+\left(\frac{U_{\rho}}{h_o}\right)T_{sol-air,M}\right]\right\}_{\rho}$. (1b)

Heat flux through a cool roof (i.e., a gray roof with cool coating applied on top) can be modelled (based on the heat transfer model [28-29]) by,

$$q_{\rho^*}^{CRHT} = U_{\rho^*}\,(1+\nu)\left\{T_{sol-air}^{S} - \left[T_i\left(1-\frac{U_{\rho^*}}{h_o}\right)+\left(\frac{U_{\rho^*}}{h_o}\right)T_{sol-air,M}\right]\right\}_{\rho^*} \tag{2}$$

$$= U_{\rho^*}\left(TD_{\rho^*}^{eqv}\right) \tag{2a}$$

where $\left(TD_{\rho^*}^{eqv}\right) = (1+\nu)\left\{T_{sol-air}^{S} - \left[T_i\left(1-\frac{U_{\rho^*}}{h_o}\right)+\left(\frac{U_{\rho^*}}{h_o}\right)T_{sol-air,M}\right]\right\}_{\rho^*}$. (2b)

Eqs. (1) and (2) are obtained by solving the equations for conduction heat transfer through a roof section and implementing the Neumann boundary conditions. In order to derive an expression for $\bar{R}_{\rho^*}^{CRHT}$, the heat flux across the cool roof, Eq. (2a), and the gray roof, Eq. (1a) are equated. It gives

$$U_{\rho^*}.\left(TD_{\rho^*}^{eqv}\right) = U_{\rho}\,.\left(TD_{\rho}^{eqv}\right) \tag{3}$$

$$R_{\rho}\,.\left(TD_{\rho^*}^{eqv}\right) = R_{\rho^*}.\left(TD_{\rho}^{eqv}\right) \tag{3a}$$

where $R_{\rho^*} = \bar{R}_o + \bar{R}_{\rho^*}^{CRHT} + \bar{R}_{substrate} + \bar{R}_i$, (where $\bar{R}_{\rho^*}^{CRHT}$ is obtained based on our previously developed heat transfer tool [28-29])

$$R_{\rho} = \bar{R}_o + \bar{R}_{substrate} + \bar{R}_i \tag{3b}$$

Further, Eq. (3a), can be written as-

$$R_{\rho^*} = \frac{\left(TD_{\rho^*}^{eqv}\right)}{\left(TD_{\rho}^{eqv}\right)} \times R_{\rho}\,, \tag{3c}$$

$$R_{\rho^*} = F \times R_{\rho}\,, \tag{3d}$$

$$\text{where } \frac{\left(TD^{eqv}_{\rho^*}\right)}{\left(TD^{eqv}_{\rho}\right)} = F\,. \tag{4}$$

Using Eq. (3b) in Eq. (3d), it is derived as-

$$\bar{R}^{CRHT}_{\rho^*} + \bar{R}_i + \bar{R}_o + \bar{R}_{substrate} = F.\left[\bar{R}_{substrate} + \bar{R}_i + \bar{R}_o\right]. \tag{5}$$

Re-arranging Eq. (5), we get

$$\bar{R}^{CRHT}_{\rho^*} = F.\left[\bar{R}_{substrate} + \bar{R}_i + \bar{R}_o\right] - \left[\bar{R}_i + \bar{R}_o + \bar{R}_{substrate}\right], \tag{6}$$

$$\text{where } F = \frac{\left(T^s_{sol-air} - \left[T_i\left(1 - \frac{U_{\rho^*}}{h_o}\right) - \left(\frac{U_{\rho^*}}{h_o}\right)T_{sol-air,M}\right]\right)_{\rho^*}}{\left(T^s_{sol-air} - \left[T_i\left(1 - \frac{U_{\rho}}{h_o}\right) - \left(\frac{U_{\rho}}{h_o}\right)T_{sol-air,M}\right]\right)_{\rho}}. \tag{6a}$$

$$T^s_{sol-air} = T_{sol-air,M} + T^+_{sol-air}\cos(wt - \psi) \tag{6b}$$

$$T^+_{sol-air} = \sqrt{\left(\frac{1}{12}\sum_{t=1}^{24} T^e_{sol-air}.\cos(wt)\right)^2 + \left(\frac{1}{12}\sum_{t=1}^{24} T^e_{sol-air}.\sin(wt)\right)^2} \tag{6c}$$

$$T^e_{sol-air} = \frac{I_0.(1-\rho)}{h_o} + T_o - \frac{\varepsilon\, I^{IR}}{h_o} \tag{6d}$$

$$\tan(\psi) = \frac{\left(\frac{1}{12}\sum_{t=1}^{24} T^e_{sol-air}.\sin(wt)\right)}{\left(\frac{1}{12}\sum_{t=1}^{24} T^e_{sol-air}.\cos(wt)\right)} \tag{6e}$$

Eq. (6) gives the expression for the thermal resistance that is improved on the gray roof result in the heat flux same as that of through a cool roof, i.e., $\bar{R}^{CRHT}_{\rho^*}$ represents the effective thermal resistance added by the increased surface albedo provided by the cool coating. It can be observed from Eq. (6) that $\bar{R}^{CRHT}_{\rho^*}$ mainly depends on the solar air temperatures and conduction resistances of substrate. The proposed model is demonstrated using field measurements as discussed in the following section.

4. Experimental validation

4.1. Experimental procedure and data analysis

Field measurements were conducted in two side-by-side, geometrically identical vacant apartment units of a 12-storey housing complex in Singapore for validations of the results computed using the proposed numerical model. In order to characterize the thermal behavior and ensure the accuracy of the proposed model under various weather conditions, the experimental data was collected over a period of month, from which a typical sunny day and a cloudy day was selected for model prediction and validation. The cloudy day was selected from non-rainy days with lowest solar radiation profile, whereas the sunny day was selected from non-rainy days with highest solar radiation profile. Fig. 1 shows the experimental arrangements for the roof of each unit. The roof of Unit-1 was a cool roof ($\rho^* = 0.80$) and Unit-2 was a gray roof ($\rho = 0.1$), which represented the original roof of the building i.e., without a cool coating. The gray roof consists of 100-mm-thick reinforced cement concrete slab and 10-mm cement plaster. Whereas the cool roof consists of a thin layer (0.5-mm) high reflectance coating applied on the exterior of this gray roof.

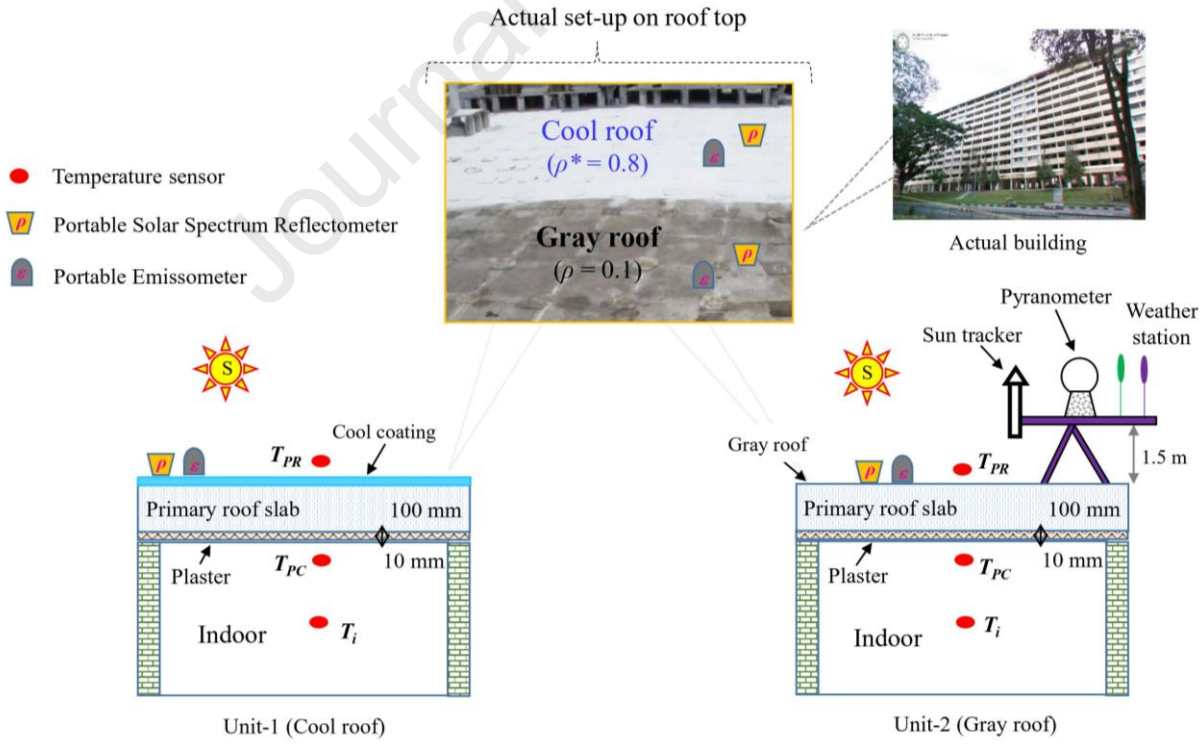

Fig. 1. Experimental arrangements for gray roof and cool roof (not-to-scale).

The weather data (ambient air temperature, wind speed, rainfall and relative humidity) was monitored using roof top weather station at the experimental site at 1-minute interval and the hourly-average of these parameters are presented in Fig. 2. A sun tracker (Solys2) connected with a pyranometer (Kipp & Zonen, CMP 11) and a pyrheliometer (Kipp & Zonen, CHP 1) with an accuracy of ±1.4% reading was used to monitor direct and diffuse solar radiation. The solar irradiation received horizontal rooftop surfaces were estimated based on these direct and diffuse components measured on site. The daily integrated solar radiation on a cloudy day was 3,860 W-h/m^2 and that of on a sunny day was 6,137 W-h/m^2. The sol-air temperature data estimated using Eqs. (6d - 6e) is shown in Fig. 2. The hourly mean of the total surface heat transfer coefficient on the respective sunny and cloudy days were estimated for both gray roof and cool roof based on the on-site measured data. RTD sensors were installed to measure the air temperature close to the roof surface. The solar reflectance and thermal emittance properties of both the roof surfaces were measured on site solar spectrum reflectometer (Devices and Services, SSR-6) and emissometer (Devices and Services, AE1-RD1).

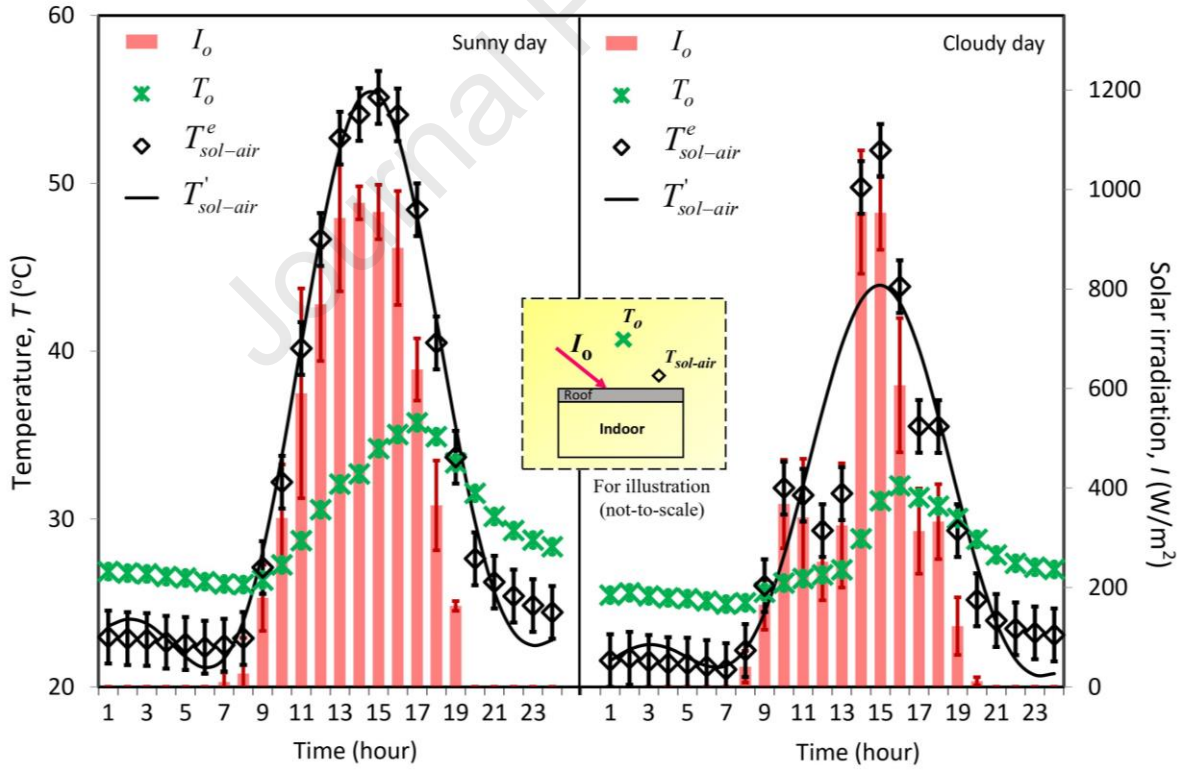

Fig. 2. Measured hourly-average outdoor air temperature (T_o), solar irradiation (I_o) and sol-air temperature ($T^e_{sol-air}$) and its Fourier series simulation ($T'_{sol-air}$) on a sunny and a cloudy day.

All the sensors and instruments were (laboratory or factory) calibrated before using for the measurements. Fig. 3a shows that the model predictions are matching with the measurements

in a reasonable margin of error. Based on the measured heat fluxes, the hourly-average effective *R* of the cool roof were estimated using

$$R^{e}_{\rho^*} = \frac{\int_{hourly} q^{e}_{\rho}\, dt}{\int_{hourly} q^{e}_{\rho^*}\, dt} \times R_{\rho} \quad \text{for cool roof,} \tag{7}$$

where $R\rho$ was obtained using Eq. (3b). Fig. 3b shows the breakdown of different thermal resistance components of cool roof (as in Eq. (3b)). The effective thermal resistance of cool roof, $R^{CRHT}_{\rho^*}$ (sum of $R^{CRHT}_{\rho} + \bar{R}^{CRHT}_{\rho^*} + \bar{R}_{coating}$), predictions (obtained using Eq. (6)) are compared with the measured effective thermal resistance of cool roof $R^{e}_{\rho^*}$. Measured R^{e}_{ρ} during nighttime becomes lower than R_{ρ} , essentially having negative $\bar{R}^{CRHT}_{\rho^*}$ values. Negative $\bar{R}^{CRHT}_{\rho^*}$ values during nighttime were also obtained by CRHT predictions. It suggests that the cool coating enhanced heat loss during nighttime (as can be observed from Fig. 3a). This could be because of higher surface air temperature difference for the cool roof when compared to the gray roof, resulting in more heat loss through the cool roof during nighttime.

A heat transfer tool developed by the authors [28-29] was used for the prediction of heat flux across the roofs. Fig. 3a shows the predicted heat fluxes of the gray roof (q^{CRHT}_{ρ}, calculated using Eqs. (1) – (1b)) and the cool roof ($q^{CRHT}_{\rho^*}$, calculated using Eqs. (2) – (2b)) on a typical sunny day as well as a cloudy day. The predictions of the numerical model are compared against the measured hourly-average heat fluxes, q^{e}_{ρ} and $q^{e}_{\rho^*}$ which were obtained from the differences between the air temperatures measured near the roof (T_{PR}) and near the ceiling surfaces (T_{PC}) of the corresponding roof slabs. On the sunny day, average error was within ± 3.2 W/m^2, whereas on the cloudy day, average error was within ± 4.6 W/m^2. In order to obtain the numerical solution using the proposed $\bar{R}^{CRHT}_{\rho^*}$ expression, inputs such as i) overall heat transfer coefficients (for each exterior and interior surface) and ii) sol-air temperature, are required. These inputs were estimated using the weather data and thermo-physical properties of the building fabric materials. Sol-air temperature combines the impact of solar irradiation, thermal radiation properties of the roofing material as well as the ambient temperature conditions (shown in Eq. (6d). The total heat transfer coeffcient (h_o) integrates the effect of both radiation ($h_{o,r}$) and convection heat transfer coefficients ($h_{o,conv}$), as

presented in Appendix (Eqs. (A-1) – (A-5)). The correlations for $h_{o,r}$ and $h_{o,conv}$ are obtained from [30] and [31], respectively. The errors of measured h_o and h_i (using temperature sensors, reflectometer, emissometer and weather station as well as employing Eqs. (A-1) – (A-9)) were ±1.4 W/m^2-K and ±0.3 W/m^2-K. The thermo-physical properties of the envelope material (shown in Table 2) were obtained from the material manufacturers [4].

Table 2. Thermo-physical properties of roof substrate materials.

Roof material	Thermal conductivity (W/m-K)	Thickness (mm)	Thermal diffusivity (m^2/s)	Volumetric heat capacity (kJ/m^3-K)
Air	0.03		1.9×10^{-5}	1.3
Plaster[a]	0.53	10	4.1×10^{-7}	1317
Reinforced concrete [a]	0.30	100	6.8×10^{-7}	2112
Plasterboard[a]	0.60	15	2.7×10^{-7}	850
Polystyrene[b]	0.08	20	1.0×10^{-6}	750
Aluminium[b]	12.5	5	5.0×10^{-6}	2500
Cool coating[a]	0.05	0.5	6.6×10^{-7}	75
PCM[c]	0.43	5	2.4×10^{-7} [s/l] / 0.9×10^{-7} [t]	1770 [s/l] / 5000 [t]

[a] Properties are provided by the manufacturers.
[b] Properties are taken from [30].
[c] Properties are taken from [3].
[s/l] Volumetric heat capacity for solid and liquid phases.
[t] Uniform effective volumetric heat capacity during the transition phase at 28^{o}C i.e., melting temperature. More information on the PCM listed can be found from our previous work [3].

4.2. Dynamic thermal performance of cool roof

The daily-integrated (or 'daily') heat ingress (during daytime) as well as heat loss (during nighttime) through both gray and cool roofs were estimated using Eqs. (8) – (9) are tabulated in Table 3.

$$Q_{\rho,gain} = \int_{daily} q_\rho dt, \quad \text{where } q \text{ is the downward heat flow.} \tag{8}$$

$$Q_{\rho,loss} = \int_{daily} q_\rho dt, \quad \text{where } q \text{ is the upward heat flow.} \tag{9}$$

Table 3. Daily integrated- heat gains and heat loss for gray and cool roof in tropical climate.

Roof	Daily integrated-heat gain (Wh/m^2-day)		Daily integrated-heat loss (Wh/m^2-day)	
	Sunny day	Cloudy day	Sunny day	Cloudy day
Gray	400	200	-86	-20
Cool	180	125	-123	-30

Table 3 suggests that the cool roof coating reduced heat ingress and increased heat loss as compared to that of the gray roof. Fig. 3b shows that the R of the gray roof, $R\rho$, remained constant throughout the whole day whereas the effective thermal resistance of the cool roof coating, $R_{\rho*}$, exhibits a dynamic nature. The effective thermal resistance of the cool roof coating comprises of three components, $\bar{R}_{\rho^*}^{CRHT}$, $\bar{R}_{coating}$ and R_ρ, where R_ρ is the R of the base gray roof substrate as defined in Eq (3b). For the cool roof, $\bar{R}_{coating}$ is essentially negligible as compared to R_ρ and $\bar{R}_{\rho^*}^{CRHT}$. Regardless of the weather conditions, R_ρ and $\bar{R}_{coating}$ remain almost constant whereas $\bar{R}_{\rho^*}^{CRHT}$ is dynamic. $\bar{R}_{\rho^*}^{CRHT}$ is highly dependent on solar irradiation and sol-air temperature (as can be observed from Eq. (6a)). $\bar{R}_{\rho^*}^{CRHT}$ during daytime is noted to be greater on a sunny day, compared to that of a cloudy day due to the reflected solar radiation. It suggests that increased solar reflectance due to cool roof coating provides more significant heat gain curbing effect to roofs subjected to more intense solar irradiation. Cool roof coating adds to the effective R_ρ during daytime as $\bar{R}_{\rho^*}^{CRHT}$ is positive. During nighttime, when there is no solar irradiation, $\bar{R}_{\rho^*}^{CRHT}$ becomes negative for most of the time which indicates that cool roof coating enhances heat loss during nighttime.

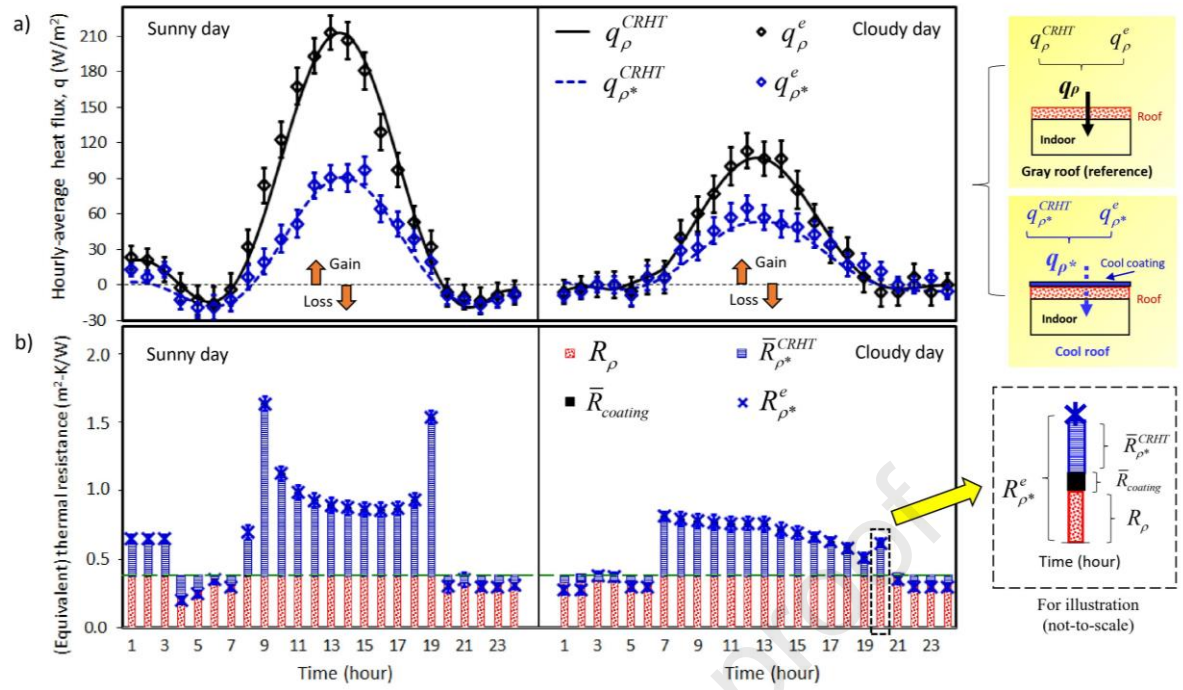

Fig. 3. Comparison of simulation and measurement results of hourly-average heat transfer and (effective) thermal resistance for gray roof and cool roof.

5. Discussion on parametric studies

Besides cool roof coating, using materials with high thermal resistance (e.g., insulation) and high volumetric heat capacity (e.g., PCM-modified skim coat (or 'PCM' hereinafter)), are also popular and emerging passive strategies to enhance thermal efficiency of building envelopes. A parametric analysis is carried out using the proposed $\bar{R}_{\rho^*}^{CRHT}$ expression to investigate the impacts of i) adding a cool roof coating (ρ increases to 0.8), ii) adding insulation (higher thermal resistance) and iii) adding thermal inertia (higher volumetric heat capacity) on the annual thermal performance of a reference gray roof (ρ = 0.1) under different climate conditions.

5.1. Insulation vs. cool coating vs. thermal inertia in tropical climate

Fig. 4 shows the predicted daily profiles of roof heat transfer to illustrate the effects of thermal inertia (C_v), solar reflectance (ρ) and thermal resistance in tropical climate (using the data shown in Fig. 2 as the climate conditions inputs). Fig. 4a shows the daily profiles of heat transfer through three gray roofs with thermal resistance of 0.25 m^2-K/W (R_1), 0.75 m^2-K/W (R_2) and 1.50 m^2-K/W (R_3). The R_1 gray roof has a thermal resistance similar to a typical insulated aluminum metal roof comprises of 5-mm aluminum + 20-mm polystyrene + 20-mm plasterboard (refer Table 4). Increasing thermal resistance (by increasing the thermal

resistance of the roof substrate, $\bar{R}_{substrate}$) leads to decrease in heat gain during daytime. For instance, increasing thermal resistance from R_1 to R_2 (effective to adding 40-mm thick of polystyrene insulation to the R_1 gray roof), decreases the daily peak heat gain by over 168 W/m^2 (≈66%) on the sunny day. In comparison, the heat gains reduction effect by increasing C_v is much less significant. For instance, for the R_1 gray roof, increasing its C_v from the original 500 (C_{v1}) to 5,000 kJ/m^3-K (C_{v2}) (similar C_v to a roof consists of 200-mm reinforced concrete, 120-mm polystyrene and 5-mm PCM layer) only reduces the peak time heat gain from 253 to 180 W/m^2 (≈29%). It can be observed from Fig. 4a that increasing C_v also leads to delay of heat gain, due to the higher thermal inertia in high-C_v roofs. The delay of heat gain results in increased heat gains during nighttime. It can be noted that the outdoor air temperature on these two days (shown in Fig. 4) is above the indoor set point temperature (24°C), resulting heat gain even during night time by increasing thermal resistance and C_v of the substrate and additionally heat gain delays when C_v is increased. The small amount of heat loss observed during night time could be mainly due to radiative loss.

Table 4. Effect of ρ, C_v and R on daily heat gain and heat loss performance in tropical climate.

Effect of substrate properties	Parameter	Daily integrated-heat gain (Wh/m^2-day)		Daily integrated-heat loss (Wh/m^2-day)	
		Sunny day	Cloudy day	Sunny day	Cloudy day
Surface radiative (Solar reflectance)	Increasing ρ only (from 0.1 to 0.8)	drop 68%	drop 60%	rise 50%	rise 43%
Thermo-physical (Volumetric heat capacity)	Increasing C_v only (from 500 to 5000 kJ/m^3-K)	drop 8%	drop 1%	drop 100%	drop 100%
Thermo-physical (thermal resistance)	Increasing R only (from 0.25 to 1.50 m^2-K/W)	drop 82%	drop 80%	drop 50%	drop 60%

Baseline gray roof: R = 0.25 m^2-K/W, C_v = 500 kJ/m^3-K and ρ =0.1.

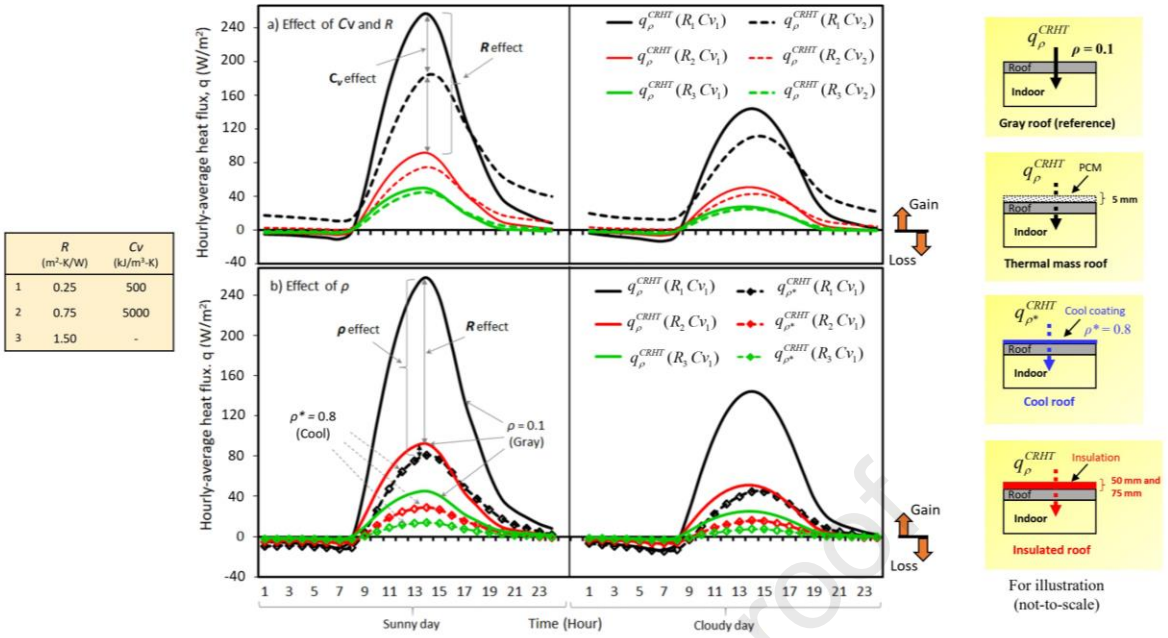

Fig. 4. Comparison of effect of C_v, ρ and R on roof heat transfer performance in tropical climate of Singapore

Fig. 4b illustrates the predicted effect of surface reflectance, ρ, of the three roofs (R_1 – R_3 with C_v of 500 kJ/m^3-K). It can be observed that adding cool coating significantly reduces heat gain without causing the delay in heat gain. Therefore, unlike the case of increasing C_v, the higher ρ does not lead to increase in heat gain during nighttime. For instance, for the R_1 gray roof, increasing ρ by 0.7 decreases the daily peak heat gain from 253 to 91 W/m^2 (≈64%), without causing increased heat gain and delay during nighttime. Therefore, the overall effect of increasing ρ on reducing daily heat gain should be much more significant than increasing C_v. To put in a practical perspective, adding a thin layer of cool roof coating on top of the R_1 substrate is essentially equivalent to adding a 40-mm of polystyrene insulation, in terms of reduction in daily heat gain. The predicted impacts of different C_v, thermal resistance and ρ on daily heat flow through the roofs are summarized in Table 4. Increasing C_v from C_{v1} to C_{v2} leads to only 8% daily heat gain reduction on a typical sunny day as compared to 68% reduction due to adding cool roof coating and 82% reduction due to increasing thermal resistance from R_1 to R_3. These findings highlight that increasing thermal inertia of the roof is less effective in reducing daily heat ingress than adding insulation or adding cool roof coating. It can also be observed that the effect of C_v in reducing and delaying peak heat gain further reduces with the increase in thermal resistance of the roof substrate.

Fig. 5 shows the impact of C_v, ρ and thermal resistance estimated on yearly integrated (or 'annual' hereafter) heat ingress and respective effective thermal resistances. The annual predictions were based on typical metrological year (TMY) data of Singapore [32]. The sol-air temperature profiles (required input to the proposed model) are estimated using the detailed expressions given in [28]. Fig. 5a shows that, for roofs with the range of thermal resistance shown, increase in C_v leads to a much smaller (< 5%) reduction in annual heat ingress, when compared to the reductions achieved by increasing ρ or thermal resistance (60 – 80%). Taking insulated (with 20-mm extruded polystyrene) gray aluminum metal roof (R 0.25 m^2-K/W and C_v 500 kJ/m^3-K) as reference, improving R by 0.5 m^2-K/W (e.g., 40-mm Polystyrene) decreases the annual heat gain by about 66%. Adding cool coating on the same reference roof (increase ρ from 0.1 to 0.8) instead decreases the annual heat gain by about 78%. However, increasing C_v to 5,000 kJ/m^3-K (e.g., by adding a 5-mm thick PCM embedded cement plaster to insulated gray aluminum metal roof (with 20-mm polystyrene)), the annual heat gain reduces only by about 2%.

Fig. 5b shows the effective thermal resistance of cool roofs corresponding to those shown in Fig. 5a. The total height of each stack indicates the effective thermal resistance of the high albedo cool roof. Each stack consists of the components of the thermal resistance of the base roof substrate, the effective thermal resistance of the cool surface ($\bar{R}_{\rho^*}^{CRHT}$) and the thermal resistance of the layer of cool paint ($\bar{R}_{coating}$). The contribution of $\bar{R}_{coating}$ to the effective thermal resistance of cool roof, $R_{\rho^*}^{CRHT}$, is negligible in this case as the cool coating is very thin (i.e., 0.5-mm). It indicates that most of the heat reduction due to cool surface is coming from its high solar reflectance. In contrast, rising thermal inertia from 500 to 5,000 kJ/m^3-K shows an insignificant effect on the effective thermal resistance across the range of different R shown in Fig. 5b.

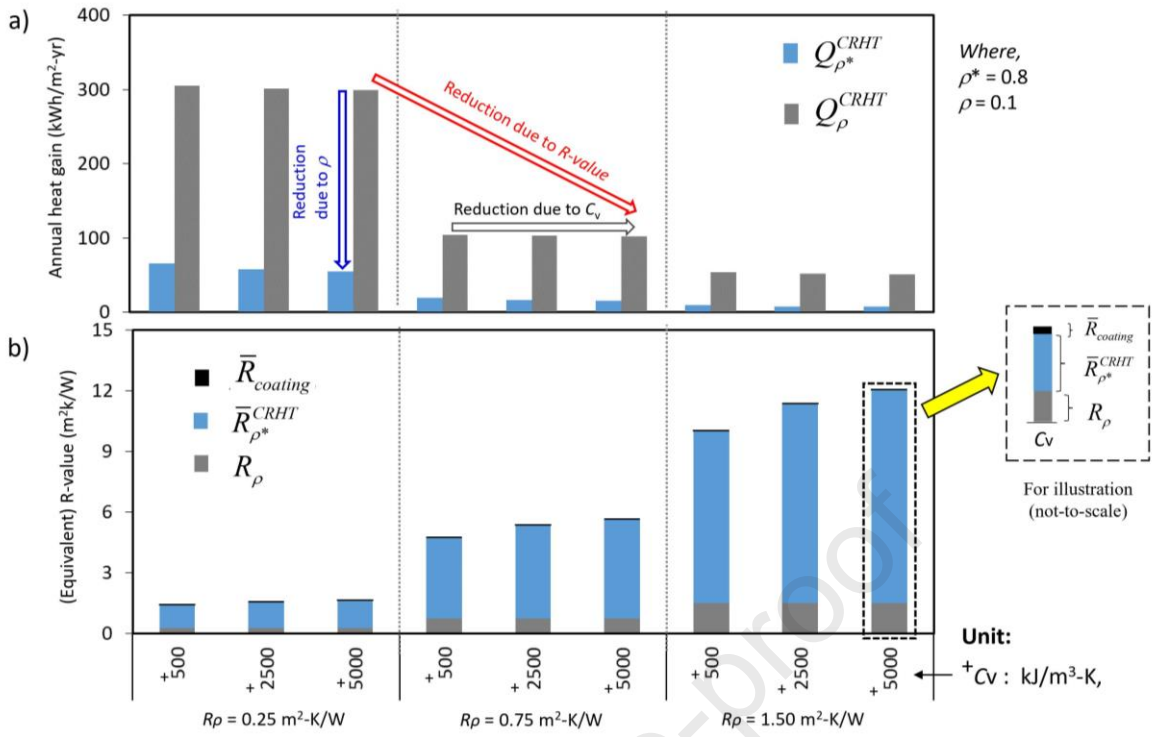

Fig. 5. Comparison of effect of C_v, ρ and R on the annual thermal performance of a gray roof in tropical climate of Singapore.

The predicted effects of thermal resistance, heat capacity and surface reflectance on the annual heat ingress and effective thermal resistance therefore are summarized in 3D contour graphs in Fig. 6. Commonly used roof constructions (Table 5) are marked on these plots. It is evident from Fig. 6a that decrease in annual heat ingress (shown by color contours) with increase in reflectance is prominent for the less insulated roofs. In comparison, increase in thermal inertia has much smaller impact in the reduction of annual heat ingress. This is similar to the observations from Figs. 4 and 5, where increase (effective) thermal resistance, either by adding an insulation material or by adding a cool coating, offers a better solution for reduction in roof heat gain as compared to adding thermal inertia. Fig. 6 also highlights that adding cool coating is effective for original roof having low ρ and adding insulation material for high ρ roofs becomes even more effective. Fig. 6 can generally be used for roofs having thermal resistance from 0.25 to 3.00 m^2-K/W with C_v < 5,000 kJ/m^3-K and ρ between 0.1 and 0.9 to estimate the reduction in annual heat ingress and change in (effective) R in tropical climates. The values of (effective) R can be further used for the estimation of Roof Thermal Transfer Value, RTTV [33] using Eqs. (A-10) and (A-11), in Appendix. Table 6 shows the improvements in RTTV estimation of various commonly used roof assembly by the use of the proposed $R^{new}_{\rho^*}$ model as compared to the existing model.

Table 5. Thermo-physical properties of roof substrate materials.

Roof assembly				Symbol in Fig. 6	R (m^2-K/W)	ρ of exterior surface	Volumetric heat capacity (kJ/m^3-K)
No.	External layer	Middle layer	Internal layer				
1	Aluminum sheet (5-mm)	Polystyrene (20-mm)	Plaster (20-mm)	✚	0.25	0.10	500
2	Aluminum sheet* (5-mm)	Polystyrene (20-mm)	Plaster (20-mm)	□	0.25	0.60	500
3	Cement concrete (200-mm)	Polystyrene (30-mm)	Plaster (15-mm)	△	0.75	0.10	2,300
4	Cement concrete (200-mm)	Polystyrene (40-mm)	Plaster (15-mm)	○	0.85	0.10	2,100
5	Cement concrete (200-mm)	Polystyrene (120-mm)	PCM (5-mm)	☆	1.50	0.10	1770 [s/l] / 5000 [t]
6	Aluminum sheet (5-mm)	Polystyrene (120-mm)	Plaster (20-mm)	⧖	1.50	0.10	3,500

*****Metal roof with high ρ = 0.60 (without cool coating).
[s/l] Volumetric heat capacity for solid and liquid phases
[t] Uniform effective volumetric heat capacity during the transition phase at 28°C i.e., melting temperature. More information on the used PCM can be found from our previous work [3].

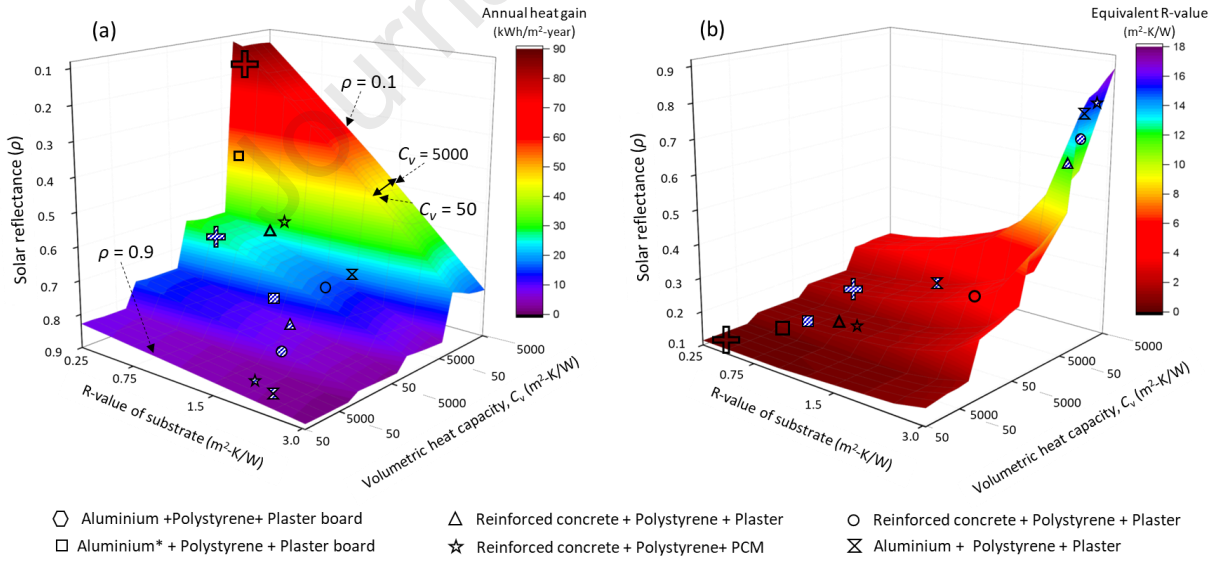

Fig. 6. 3D plot showing the effects of C_v, R and ρ on (a) annual heat gain and (b) effective R-value for roof assemblies (see Table 4) in tropical climate (striped symbols represent roof substrate having cool coating, i.e., ρ = 0.8 and unstriped ones represent gray roof surface i.e., ρ = 0.1).

Table 6. Comparison of *RTTV* of common roof assembly substrate materials (with cool coating) obtained using Existing approach vs proposed approach.

Roof assembly substrate materials with cool coating (symbol taken from Fig. 6 and Table 5)	*RTTV* (opaque portion of the roof) = $\frac{TD_{eq}}{R_{\rho^*}}$ i.e., Eq. (A-11) in Appendix		Error (%)
	$\frac{12.5}{R_{\rho^*}}$ (Existing)	$\frac{12.5}{R_{\rho^*}^{new}}$ (Proposed)	
✠	50	11	78
□	21	11	48
△	17	5	71
◯	15	4	73
☆	8	2	75
⧖	8	2	75

5.2. Insulation vs. cool coating vs. thermal inertia in various climates

The predicted impacts of thermal resistance, C_v and ρ on annual thermal performance of a reference gray roof are further investigated in four different climates (shown in Figs. 7 and 8): 1) hot and humid tropical represented by Singapore, 2) hot dessert represented by Abu Dhabi, 3) composite represented by Delhi and 4) Mediterranean represented by Barcelona. The TMY weather data of these four selected cities are taken from [32]. The inputs required for the model predictions such as solar irradiation, sky temperature and heat transfer coefficients are shown in Table 7. Fig. 7 presents (maximum, mean and minimum) monthly average ambient air temperature, whereas Fig. 8 presents annual diurnal temperature variation and sky temperature across the selected four climates. The maximum monthly average air temperature in the three tropical cities (Singapore, New Delhi and Abu Dhabi) are above indoor set point temperature (24°C) throughout the year and monthly mean temperature profiles for at least 8 months, whereas for Barcelona, the maximum monthly outdoor air temperature profile is above 24°C only for 4 months (i.e., March-June).

Table 7. Thermal resistance of air film on ceiling and roof surfaces and weather parameters in various climate conditions.

Location (climate)	$^{*}\bar{R}_o$ (m^2-K/W)	$^{*}\bar{R}_i$ (m^2-K/W)	$^{\times\times}I_o$ (kWh/m^2-year)	$^{\times}T_o$ (°C)	$^{\times}T_{sky}$ (°C)	$^{\times}\Delta T$ (°C)
Singapore	0.031	0.234	1831	27.5	18.1	5.7
Abu Dhabi	0.032	0.237	2896	27.1	14.9	11.9
New Delhi	0.033	0.240	2572	24.5	12.3	11.5
Barcelona	0.031	0.228	1938	15.7	3.7	7.4

$^{\times}$Annual-average parameters.
$^{\times\times}$Annual integrated parameters.
$^{*}\bar{R}_i$ and $\bar{R}_o$ are obtained using expressions given in [20].

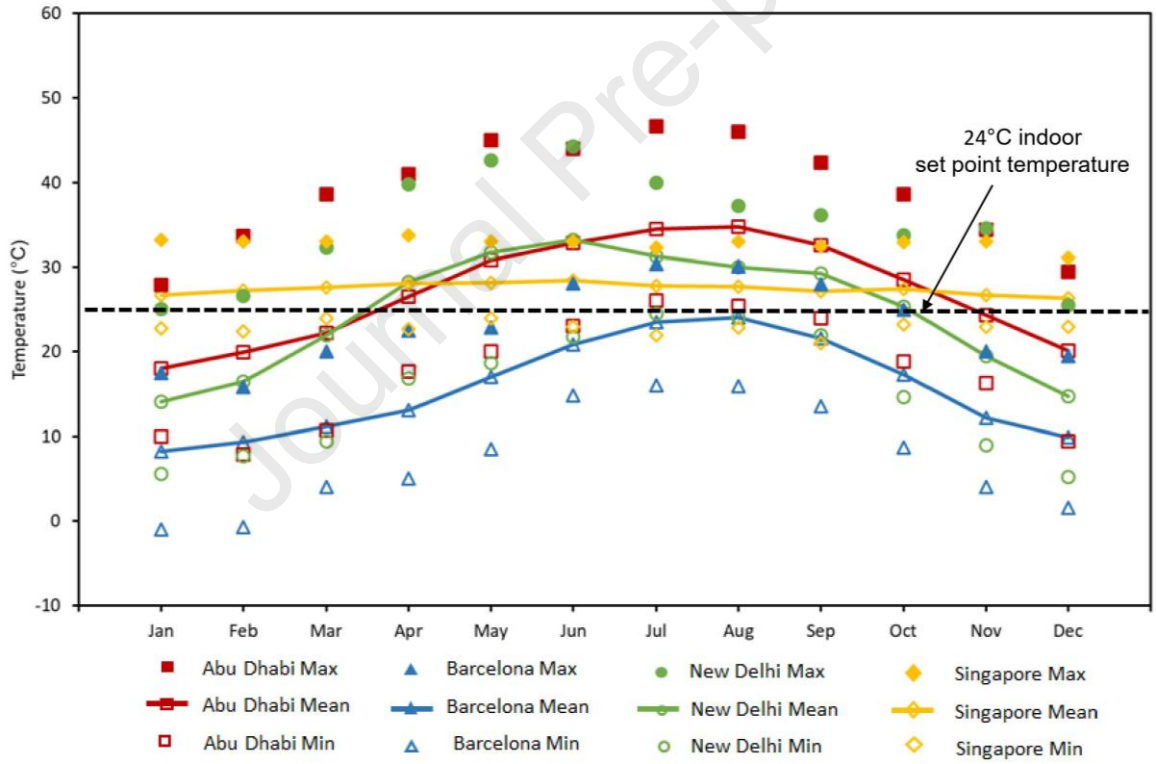

Fig. 7. Monthly-averaged outdoor air temperatures at the selected four cities.

Fig. 9a presents the annual heat gain and Fig. 9b shows the corresponding effective thermal resistance increment with varying thermal resistance, C_v and ρ in all the four climates. It can be noted that the amount of annual heat flux changes with the ambient climatic conditions. In general, the comparison of annual heat flux performance reveals that the effects of varying thermal resistance (between 0.25 and 1.5 m^2-k/W), C_v (between 500 and 5000 kJ/m^3-K) and ρ

(between 0.1 and 0.8) separately are almost same i.e., 83%, 2-4% and 78%, respectively in Singapore, Abu Dhabi and New Delhi, where building cooling is sought almost throughout the year.

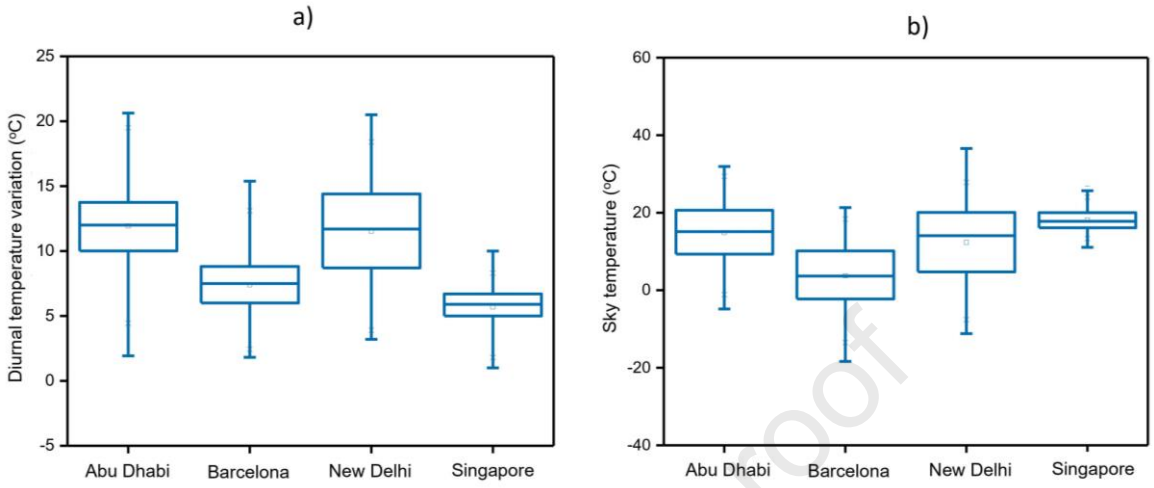

Fig. 8. Annual statistics of diurnal temperature variation and sky temperature across the selected four climates (TMY).

However, the performance of high albedo and thermal inertia (C_v) in the Mediterranean climate of Barcelona is found to be prominent (i.e., 96% and 22%, respectively). The total annual heat flux across the reference gray roof in Barcelona (see Fig. 9a) is significantly lower (50%) than that of the other three climates and that through a cool roof is almost zero. This could be due to the effect of distinct climate characteristics of Barcelona as compared to in other three climates; the lower outdoor air and sky temperatures cause lower temperature difference across the roof, resulting negligible annual heat gain across the cool roof. Table 5 and Fig. 8b illustrate that the annual mean sky temperature in Barcelona is 3.7°C whereas the same is in the range of 12.3°C – 18.1°C in other three climates. Thus, the lower sky temperature is resulting more radiative heat loss of the stored heat in Barcelona in contrast with the other three tropical climates, demonstrating higher effect of increase in C_v. The effect of thermal resistance of the substrate material on annual heat gain reduction is found to be more or less same (82-83%) in all the four climates.

Table 8 summarizes the heat curbing effects of individual parameters i.e., increasing ρ or C_v or thermal resistance, as well as their combined effect on the decrease of annual heat flux. For a cool roof, the effect of increasing R (i.e., insulation) on the decrease of annual heat flux is only 3% for Barcelona compared to 19-24% reduction in the other three climates. The majority of annual heat gain reduction i.e., 96% in Barcelona is achieved just by increasing ρ of the roof. However, the effect of increasing thermal inertia for a high ρ substrate leads no

significant reduction (1-4%) regardless of the climate. Thus, it can be summarized that, to curb the heat gain through the roof, the effect of adding thermal resistance is beneficial only in cooling dominated climates like Singapore, Delhi and Abu Dhabi. And the effect of adding C_v is not so prominent once the high reflective roof strategy has been implemented.

Table 8. Summary of annual heat gain reduction for various cases studied in this paper.

Location (climate)	ρ (0.1 to 0.8)	C_v (500 to 5000)	R-value (0.25 to 1.5)	$\rho + C_v$	$\rho + R$	$\rho + C_v + R$
Singapore	78%	2%	83%	82%	97%	98%
Abu Dhabi	73%	2%	83%	74%	96%	96%
New Delhi	79%	4%	83%	80%	97%	97%
Barcelona	96%	22%	82%	98%	99%	100%

Unit of C_v is kJ/m^3-K
Unit of R is m^2-K/W

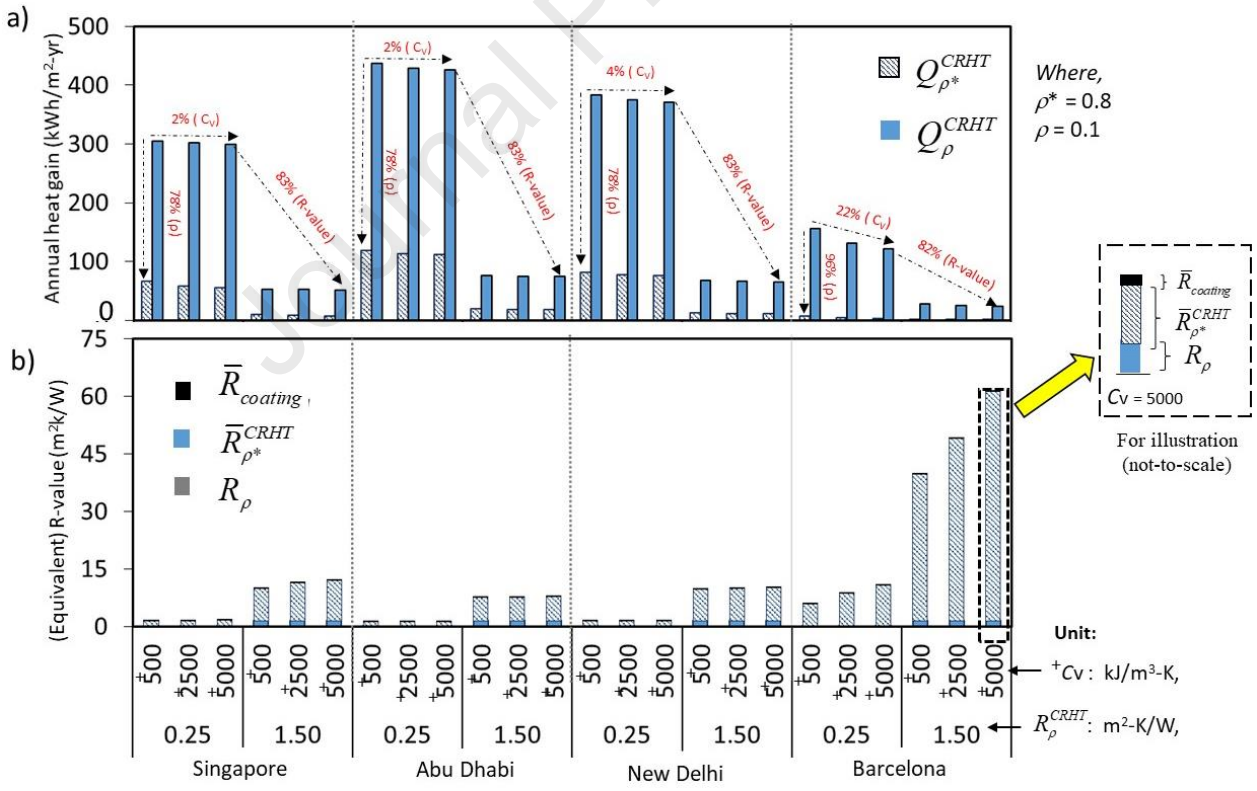

Fig. 9. Comparison of effect of C_v, ρ and R on the annual thermal performance of a gray roof in four different climate conditions.

6. Conclusions

Some existing building guidelines/codes regulate the thermal efficiency of building envelope by specifying the steady-state thermal resistances of substrate material. These guidelines/codes do not necessarily reflect the dynamic thermal behaviour of some passive strategies such as surface reflectance and thermal mass (e.g., cool and phase change materials). The concept of effective thermal resistance based on surface radiative and thermo-physical properties could facilitate the effectiveness of using passive substrate materials. Novel and simple to use single performance factor, $\bar{R}_{\rho^*}^{CRHT}$ is derived for effective thermal resistance estimation and is validated against measurements performed on two adjacent apartment units of a 12-storey housing complex. Increased solar reflectance due to cool coating is observed to be dynamic in nature and makes major contribution to the envelope's effective thermal resistance. In hot and humid climate, it is found that by increasing roof reflectance (from 0.1 to 0.8) the daily heat gain reduces by 60-68%, and by increasing the resistance of the roof (from 0.25 to 1.50 m^2-K/W) daily heat gain reduces by 80-82% whereas increasing the volumetric heat capacity (from 500 to 5000 kJ/m^3-K) reduces the daily heat gain only by 1-8%. The effect of adding a cool coating (increasing reflectance from 0.1 to 0.8) for an insulated gray aluminum metal roof (with 20-mm polystyrene) is almost effective to further adding thermal resistance of 0.50 m^2-K/W or 40-mm polystyrene. It is also observed that the effect of adding cool coating reduces as the solar reflectance value of the reference roof increases.

Furthermore, the effect of envelope properties (surface radiative and thermo-physical such as insulation and thermal inertia) is investigated using the proposed model for different climate conditions (hot and humid, dessert, composite and Mediterranean). It is found that in the hot climate, increasing reflectance alone has advantages during both daytime (in reducing heat gain) and nighttime (in allowing heat loss), however increasing thermal resistance or thermal inertia individually has advantage only during daytime, but penalty during nighttime. Increasing R provides the highest savings of about 82-83%, followed by increasing reflectance of about 73-79% and the least for increasing thermal inertia of about 2-4%. While addressing at the combined effect of the passive heat reduction strategies, increasing $\rho + R$ of the envelope is found to have 15-22% more heat gain reduction in hot climates than increasing just $\rho + C_v$. Among all the four different climates simulated, performance of high reflectance and thermal inertia is found to be substantial in the Mediterranean climate of Barcelona because of the lower ambient temperatures. Apart from being concise and easy to

use, the proposed model has real world applications for the estimation of envelope thermal efficiency indicator such as roof thermal transfer value of substrate assemblies integrated with cool and phase change materials and not constrained by climate conditions. In future, this work will be beneficial for: 1) quick and simple comparison of effectiveness of various passive strategies at the early design stage based on a single factor, 2) accurate estimation of thermal efficiency of opaque roof and wall assemblies integrated with cool and phase change materials, and 3) designing policies for management of building loads.

Acknowledgements

This research was financially supported by the Housing & Development Board, Singapore. Technical and logistical support by Energy Research Institute at NTU (ERI@N) and the Hong Kong Research Grant Council via Collaborative Research Fund (CRF) account C6022-16G are gratefully acknowledged.

Glossary

ASHRAE	American Society of Heating Refrigeration and Air-conditioning Engineers
BCA	Building and Construction Authority of Singapore
CRHT	Cool Roof Heat Transfer model
EPBD	Energy Performance in Buildings Directive
PCM	Phase change material-modified skim coat
RTTV	Roof Thermal Transfer Value
R-value, R	Overall thermal resistance (m^2-K/W)
$\bar{R}$	Thermal resistance (m^2-K/W)
SKR	Skylight ratio
TMY	Typical Meteorological Year (includes weather data on an hourly basis)
U-value, U	Overall heat transfer coefficient (W/m^2-K)

Nomenclature

C	Heat capacity {J/kg-K}
C_V	Volumetric heat capacity {kJ/m^3-K}
C_{air}	Thermal specific heat capacity of air, {J/kg-K}
D_h	Hydraulic diameter {m}
F	Intermediate variable
$\hat{F}$	Shape factor
h_i	Overall heat transfer coefficient of ceiling surface {W/m^2-K}
h_o	Overall heat transfer coefficient of roof surface {W/m^2-K}

I_o	Solar irradiation {W/m^2}
L_{gap}	Height of air gap {m}
L_i	Height of indoor {m}
L_{SR}	Thickness of secondary roof {m}
L_{PR}	Thickness of primary roof {m}
q_{ρ}^{CRHT}	Predicted heat flux through a gray roof using the CRHT model{W/m^2}
$q_{\rho^*}^{CRHT}$	Predicted heat flux through a cool roof using the CRHT model {W/m^2}
q_{ρ}^{e}	Measured heat flux through a gray roof {W/m^2}
$q_{\rho^*}^{e}$	Measured heat flux through a cool roof {W/m^2}
Q_{loss}	Heat loss (integrated-hourly upward conduction heat flux) {kW-h/m^2}
Q_{gain}	Heat gain (integrated-hourly downward conduction heat flux) {kW-h/m^2}
R	R-value of a roof (m^2-K/W)
$\bar{R}$	Thermal resistance of a roof (m^2-K/W)
R_{ρ}	R-value of gray roof {m^2-K/W}, $R_{\rho} = K_o + K_{substrate} + K_i$
R_{ρ^*}	Effective R-value of cool roof {m^2-K/W}, $R_{\rho^*} = K_o + K_{\rho^*}^{CRHT} + K_{substrate} + K_i$
$\bar{R}_{\rho^*}^{CRHT}$	Effective thermal resistance due to solar reflectance {m^2-K/W}
$\bar{R}_i$	Thermal resistance of air film on ceiling surface indoors {m^2-K/W}
$\bar{R}_o$	Thermal resistance of air film on roof surface outdoors {m^2-K/W}
$\bar{R}_{coating}$	Thermal resistance of cool coating {m^2-K/W}
$\bar{R}_{substrate}$	Thermal resistance of substrate material {m^2-K/W}
t	Time {hour}
T_{PC}	Primary ceiling temperature {K}
T_{PR}	Primary roof temperature {K}
T_{SC}	Secondary ceiling temperature {K}
T_{SR}	Secondary roof temperature {K}
T_{sky}	Sky temperature {K}
$T_{sol-air}^{e}$	Sol-air temperature obtained from experiment{K}
$T_{sol-air}^{'}$	Fourier-series simulated sol-air temperature {K}
$T_{sol-air,M}^{'}$	Daily mean sol-air temperature {K}
$TD_{\rho^*}^{eqv}$	Effective temperature difference for the cool roof {K}
TD_{ρ}^{eqv}	Effective temperature difference for the gray roof {K}
T_i	Indoor air temperature {K}
T_o	Outdoor air temperature {K}
ΔT	Mean diurnal temperature range {K}
U_{ρ^*}	Overall *U*-value of cool roof {W/m^2-K}
U_{ρ}	Overall *U*-value of gray roof {W/m^2-K}

Greek symbols

α	Thermal diffusivity {m^2/sec}
ε	Thermal emittance ($0 < \varepsilon < 1$)

ρ	Solar reflectance ($0 < \rho < 1$)
σ	Stefan-Boltzmann constant

Subscripts

c	Convection
*ρ**	Cool roof (substrate material + cool coating (on top))
g	Ground
i	Indoor
loss	Heat loss
M	Mean
o	Outdoor
PC	Primary ceiling
PR	Primary roof
r	Radiative
SC	Secondary ceiling
SR	Secondary roof
sol-air	Solar-air
v	Volumetric

Superscripts

CRHT	Cool Roof Heat Transfer model
e	Experimental
eqv	Effective
IR	Infrared radiation
s/l	Solid and liquid phases of PCM
t	Transition phase of PCM
+	Intermediate variable

References

[1] Ming CY, Ming KY , Lip HS, Tan CN, Kah PC , Durairaj R, Jing HB. Experimental analysis on the active and passive cool roof systems for industrial buildings in Malaysia. Journal of Building Engineering 2018; 19:134-141.

[2] Kiran Kumar DEVS, Puranik S. Thermal performance evaluation of a mineral-based cement tile as roofing material. Indoor and Built Environment 2015;26,409-421.

[3] Yang LJ, Kumarsamy K, Zingre KT, Yang J, Wan MP, Yang EH. Cool colored coating and phase change materials as complementary cooling strategy for building cooling load reduction in tropics. Applied Energy 2017;190:57–63.

[4] Zingre KT, Wan MP, Wong SK, Toh WBT, Lee IYL. Modelling of cool roof performance for double-skin roofs in tropical climate. Energy 2015a;82:813-826.

[5] Zingre KT, Wan MP, Yang X. Performance analysis of cool roof, green roof and thermal insulation on a concrete flat roof in tropical climate. Evergreen: joint journal of Novel Carbon Resource Sciences & Green Asia Strategy 2015b:2; 34-43.

[6] Kosny J, Petrie T, Gawin D, Childs P, Desjarlais A, Christian J. Energy Benefits of application of massive walls in residential buildings. Thermal Performance of the Exterior Envelopes of Whole Buildings VIII, ASHRAE, 2001.

[7] Zingre KT, Wan MP, Yang X. A new RTTV (Roof thermal transfer value) model for cool roofs. Energy 2015c:81; 222-232.

[8] Muscio A, Akbari H, An index for the overall performance of opaque building elements subjected to solar radiation. Energy and Buildings 2017;157:184-194.

[9] Chan ALS, Chow TT. Evaluation of Overall Thermal Transfer Value (*OTTV*) for commerical buildings constructed with green roof. Applied Energy 2013;107:10-24.

[10] Devgan S, Jain AK, Bhattacharjee B. Predetermined overall thermal transfer value coefficients for composite, hot-dry and warm-humid climates, Energy and Buildings 2010;42:1841-1861.

[11] Kotsiris G, Androutsopoulos A, Polychroni E, Nektarios PA. Dynamic U-value estimation and energy simulation for green roofs. Energy and Buildings 2012; 45:240-249.

[12] Cabeza L, et al. Experimental study on the performance of insulation materials in Mediterranean construction. Energy and Buildings 2010; 42:630-636.

[13] Stazi F, Tomassoni E, Bonfigli C, Di Perna C. Energy, comfort and environmental assessment of different building envelope techniques in a Mediterranean climate with a hot dry summer. Applied Energy 2014;134:176–196.

[14] Li P, Qiang X, Yue N, Tong Q. Analysis of climate adaptive energy-saving technology approaches to residential building envelope in Shanghai. Journal of Building Engineering 2018; 19:266-272.

[15] Di Perna C, Stazi F, Casalena AU, D'Orazio M. Influence of the internal inertia of the building envelope on summertime comfort in buildings with high internal loads. Energy and Buildings 2011; 43:200-206.

[16] Mavromatidis L. Constructal macroscale thermodynamic model of spherical urban greenhouse form with double thermal envelope within heat currents. Sustainability 2019;11:3897.

[17] Mavromatidis L. Coupling architectural synthesis to applied thermal engineering, constructal thermodynamics and fractal analysis: An original pedagogic method to incorporate "sustainability" into architectural education during the initial conceptual stages. Sustainable Cities and Society 2018;39:689-707.

[18] Mavromatidis L. Study of coupled transient radiation-natural convection heat transfer across rectangular cavities in the vicinity of low emissivity thin films for innovative building envelope applications Energy and Buildings 2016;120:114-134.
[19] Mavromatidis L. A review on hybrid optimization algorithms to coalesce computational morphogenesis with interactive energy consumption forecasting, Energy and Buildings 2015; 106:192-202.
[20] Mavromatidis L, Bykalyuk A, Lequay H. Development of polynomial regression models for composite dynamic envelopes' thermal performance forecasting. Applied Energy 2013;104:379-391.
[21] Bejan A, Lorente S. Design with constructal theory. New Jersey, USA: Wiley. 2008.
[22] Bejan A, Peder Zane J. Design in nature. New York, USA: Anchor Books 2013.
[23] Muriel A. Reversibility and irreversibility from an initial value formulation. Physics Letters A 2013;377:1161-1165.
[24] Bejan A. The physics of life: the evolution of everything. New York: St. Martin's Press. 2016.
[25] Zhang Y, Zhang Y, Wang X, Chen Q. Ideal thermal conductivity of a passive building wall: Determination method and understanding. Applied Energy 2013;112, 967–974.
[26] Zhang Y, Chen Q, Zhang Y, Wang X. Exploring buildings' secrets: The ideal thermophysical properties of a building's wall for energy conservation. International Journal of Heat and Mass Transfer 2013;65, 265–273.
[27] Long L, Hong Y. The roles of thermal insulation and heat storage in the energy performance of the wall materials: a simulation study. Scientific Reports 2016. DOI: 10.1038/srep24181.
[28] Zingre KT, Yang EH, Wan MP. Dynamic thermal perfomance of inclined double-skin roof: Modeling and experimental investigation. Energy 2017;133:900–912.
[29] Zingre KT, Wan MP, Tong S, Li H, Chang W-C, Wong SK, Toh WBT, Lee IYL. Modeling of cool roof heat transfer in tropical climate. Renewable Energy 2015;75:210-223.
[30] Suehrcke H, Peterson EL, Selby N. Effect of roof solar reflectance on the building heat gain in a hot climate. Energy and Buildings 2008;40(12):2224-2235.
[31] McAdams WH. Heat transmission. 3rd ed. New York: McGraw-Hill; 1954.
[32] EnergyPlus Weather Dataset. Typical meteorological year weather data files for EnergyPlus simulations, U.S. Department of Energy, University of Illinois; 2013.
[33] Code on Envelope Thermal Performance for Buildings, Building and Construction Authority of Singapore, 2008, from http://www.bca.gov.sg/PerformanceBased/others/RETV.pdf.

Appendix. Supplementary data

Estimation of overall heat transfer coefficient for roof surface (h_o)

The overall heat transfer coeffcient (h_o) combines the effect of radiation ($h_{o,r}$) and convection heat transfer coefficients ($h_{o,conv}$), as shown in Eqs. (A-1) – (A-5). The correlations for $h_{o,r}$ and $h_{o,conv}$ are obtained from [30] and [31], respectively.

$$h_o = h_{o,conv} + h_{o,r}.\frac{T_{PR} - T_{sky}}{T_{PR} - T_o} \quad \text{for a flat roof facing the sky,} \tag{A-1}$$

where

$$h_{o,conv} = 5.6 + 4.0V \text{ for } V < 4.88 \text{ m/s or}$$

$$h_{o,conv} = 7.2V^{0.78} \text{ for } V \geq 4.88 \text{ m/s,} \tag{A-2}$$

$$h_{o,r} = \varepsilon.\sigma.\widehat{F}_{R,sky}({T_{PR}}^2 + {T_{sky}}^2).(T_{PR} + T_{sky}), \tag{A-3}$$

$$\widehat{F}_{PR,sky} = 0.5(1+\cos\varphi) \quad (\widehat{F}_{PR,sky} = 1 \text{ for a horizontal surface}), \tag{A-4}$$

$$T_{sky} = 0.0552(T_o)^{1.5} \text{ for clear sky days or}$$

$$T_{sky} = T_o \text{ for cloudy sky days.} \tag{A-5}$$

Estimation of overall heat transfer coefficient for ceiling surface (h_i)

The overall heat transfer coeffcient for ceiling surface (h_i) combines the effect of radiation ($h_{i,r}$) and convection heat transfer coefficients ($h_{i,conv}$), as shown in Eqs. (A-6) – (A-9).

$$h_i = h_{i,conv} + h_{i,r} \tag{A-6}$$

where

$$h_{i,conv} = (0.704/D_h^{0.601}).(T_{PC} - T_i)^{0.33}, \tag{A-7}$$

$$h_{i,r} = \frac{\sigma.\varepsilon_i}{4\times(2-\varepsilon_i)}(1+\widehat{F}_{PC,floor})(T_{PC} + T_{floor})^3, \tag{A-8}$$

$$\widehat{F}_{PC,floor} = \sqrt{1+\frac{L_i^2}{W^2}} - \frac{L_i}{W} \qquad (\widehat{F}_{PC,floor} = 1 \text{ for } L_i << W). \tag{A-9}$$

Estimation of Roof Thermal Transfer Value (*RTTV*), obtained from [33]

$$RTTV = \left(\frac{TD_{eq}}{R_{\rho^*}} \times (1 - SKR) \right)_{opaque} + \left(\frac{4.8 \times SKR}{R_{Skylight}} \right)_{skylight} + \left(485 \times SKR \times CF \times SC \right)_{skylight} \quad \text{(A-10)}$$

$$RTTV = \frac{TD_{eq}}{R_{\rho^*}} \text{ (for the opaque portion of the roof and assuming } SKR = 0) \quad \text{(A-11)}$$

Highlights

- Analytical model to study in-depth dynamic variation in the *R*-value due to passive substrate properties.
- Generalized expression which is applicable to any envelope assembly and climatic conditions.
- The proposed method is validated against measurements on a real-scale building.
- Parametric study is performed to evaluate dynamic performance of substrates for different climatic regions.

Declaration of interests

☒ The authors declare that they have no known competing financial interests or personal relationships that could have appeared to influence the work reported in this paper.

☐The authors declare the following financial interests/personal relationships which may be considered as potential competing interests: